27th Applied Aerodynamics Conference

Wake Vortex Alleviation by Differential Flap Setting and Oscillating Flap Setting: A flight test

Guido Voss[1], Thomas Gerz[2], Robert Baumann[2], Eike Stumpf[3], Michael Press[4]

German Aerospace Center

[1] Institute of Aerodynamics and Flow Technology
Lilienthalplatz 7
D-38108 Braunschweig

[2] Institute of Atmospheric Physics
DLR Oberpfaffenhofen
D-82234 Wessling

[3] Institute of Air Transport Concepts and Technology Assessing
Eissendorfer Strasse 38
D-21073 Hamburg

[4] Flight department
D-38108 Braunschweig

I. Introduction

At large airports with high traffic volume the wake vortex problem is a considerably limitation of capacity in passenger handling. Dependent on weight of aircraft, staggering distances at take-off and landing have to be followed. The heavier the aircraft is, the larger is the distance between two starting or landing aircrafts. Hence, it shall be tried to increase the airport capacity by improving the handling of the wake vortex phenomena.
This goal may be achieved either with guidance support for pilots, or with techniques which are applied to the lift producing devices on the wing. Here, the spanwise lift distribution, is influenced in such way that the vortices, which are relatively stable in air at conditions of small disturbation are brought to a prematured decay.
This article presents two methods for early vortex decay experimentally investigated by flight testing. The first item is the Differential Flap Setting (DFS). Here, small changes in configuration of lift devices are applied, which leads to a variation of spanwise lift distribution. This generates a selected multiple-vortex-system, whose vortices interacts one another and contributes to decay the dangerous main vortices.
The second method is the Oscillating Flap Setting (OFS). Aim of this is the trigger of vortex instabilities by periodic moving of aileron and special additional flaps.
Every vortex in a vortex system has a characteristic frequency. If this frequency is triggered, resonance occurs which may lead to a vortex decay. Usually, the decay is caused by atmospheric disturbances namely side wind, shear wind or thermal wind. It is possible to accelerate this process by selected triggering of these instabilities [1].
In the flight test described in this article exclusively the behaviour of vortices with triggering of long-wavelength instabilities (e.g. Crow-instability) was observed and measured.

II. Test setup

The measurement object is a vortex system which is generated by the DLR research aircraft ATTAS (see Fig. 1). The ATTAS is a modified VFW 614 aircraft built at the Vereinigte Flugtechnische Werke in Bremen, Germany. The important point of modification is the integration of a Direct Lift Control system (DLC) into the main flap of the wing (Fig. 2). A fly-by-wire control system has been installed, which allows to deflect the DLC flaps independently by electric actuators in order to produce defined vortices. Furthermore, for this flight test some special additional modifications are applied to allow the symmetric deflection of the ailerons. Thus, the ailerons can be included to the vortex manipulation.

The flight parameters and flight patterns are fixed after the analysis of the weather data on flight day. Here, flight levels are chosen which have a preferably small shear wind activity. Furthermore, a flight area is defined where the thermal conditions are most capable.
The vortices produced by the ATTAS aircraft are made visible with smoke, which comes from a smoke generator mounted on the left wing. Before flight test, the smoke pod is tested on ground with different smoke oils to achieve a maximal visibility of the vortices (see Fig. 3). The measurements are conducted by an airbourne LIDAR (light detection and ranging) facility mounted on a Dassault Falcon. The LIDAR system works similar to a RADAR system, but it uses laser light instead of radio waves. LIDAR is used for measurements of atmospherical behaviour, in this special case the LIDAR facility measures circulation and sinking rates of vortices. During the flight test the Falcon aircraft was about 1000 m above the ATTAS aircraft because the LIDAR facility can only detect the area below the aircraft. Figure 4 and 5 show the schematic view of the flight pattern which was chosen on flight day. Additionally, a video tape was taken to make the ring structure visible, which is typical, if the Crow instability is triggered. The videos are also used to measure the distance of gaps in the vortex in order to deduce statistical analysis concerning correlations to the trigger frequency.
The flight speed of ATTAS with the smoke pod is limited to about 80 m/s. The Falcon aircraft with the LIDAR facility overhauls the vortex generating ATTAS aircraft with a velocity of 130 m/s and measures the vortex system from high to low vortex age. The measured distance here is about 10000 m. The advantage of this procedure is that the time of vortex visibility is maximal.
In total, four flight tests with 22 test runs were conducted. The first three flights have six measurement runs (legs) per test whereas the fourth flight had four legs due to nightfall. All flight test configurations, which are listed in Tab. 1, were almost evenly distributed to the test flights. This fact ensures that one configuration is tested with all atmospheric conditions, which are changing in the course of the day. Moreover, all configurations are measured at one atmospheric condition at a defined time of the day.

III. Configurations

In this flight test four different configurations of flap and aileron deflections were investigated. The baseline configuration is chosen as a configuration with all relevant lifting wing devices are in neutral position.
The second configuration identified as “07” includes only the movement of inboard and midboard DLC flaps. The outboard DLC flap is deflected in a fixed position, the aileron stays in neutral position. This configuration was already performed in a previous flight test which was performed only with ground video equipment [2].
The third configuration (denoted as “11”) includes the effect of aileron in Differential Flap Setting (DFS). Here, the aileron and the outboard DLC flap are statically deflected whereas the inboard DLC flaps are moved periodically.
At last, the fourth configuration (“16”) is a configuration with pure Oscillating Flap Setting (OFS). All devices including the aileron are moved periodically.
The choice of deflection angles of the ailerons and the DLC flaps has been mainly focused on lift neutrality. This means that separately on each wing segment with deflectable devices the lift is calculated. The summation of the lift forces has to be equal to the total lift force, if all devices are in neutral position. This shall largely avoid pitching motion of the aircraft during the experiment. Furthermore, no pilot intervention on the aircraft control is provided.
The maximum deflection of the ailerons is limited to ±10°. Due to the aerodynamic drag of the aileron deflection taps the real deflection is in the range of ±8° (Fig. 6).
The OFS triggering frequency was 0.5 Hz which was the most promising value obtained in a previous flight test with similar boundary conditions [2]. Tab. 1 presents the four test configurations and Fig. 6 shows the realized movements of DLC flaps and the ailerons of configuration “16” during the flight test.

IV. Results

The analysis of the investigations is divided into two parts. In the first part the results from the LIDAR measurements are shown (Fig. 7 – 14). These are particularly the decrease of the circulation with increasing vortex age and the sinking rate of the vortex system against the time.
The characteristics of the measurement data are splitted depending on wind direction (headwind, tailwind). Furthermore, the OFS- and the DFS-configurations (07, 11, 16) are shown in comparison to the baseline configuration.
The second part of the examination deals with the statistical analysis of the video tapes. Based on the velocities of the vortex generating aircraft (ATTAS) and the measurement aircraft (Falcon), the temporal distances between the gaps of the vortex system and with it the distances of the starting points of the vortex segments are measured (see Fig. 5). Whenever, from perspective of the video camera, the beginning of a vortex section passes an imaginary line, the time was kept. From

that list of timestamps the temporal distances are evaluated.

Sometimes the visibility of the vortex becomes poor due to the diffusion of the smoke. This leads to the fact, that some segments are not counted and, following from that, some vortex segments have the wrong length. This may lead to an error in the evaluation of the distribution of the relative occurence of vortex segment lengths but this could be disregarded since the number of such kind of count errors is small.

Figure 15 shows screenshots to clarify the appearance of the vortex segments, Fig. 16 – 19 shows the distribution of the relative occurence of the lengths of the vortex segments. This is relative to the total number of vortex segments for one configuration.

In Fig. 7 one can see the decrease of the circulation depending on the vortex age for the baseline configuration. The characteristics of the measurement data are relatively closed to each other. This indicates a small atmospheric influence on the vortex system. The reduction of the circulation is between 35% and 40%.

With respect to the reduction of the circulation the configuration 07 shows no significant results (Fig. 8). The change in the circulation characteristics is about 35% at wind direction 150° (headwind) and about 45% at wind direction 330° (tailwind). Particularly at flight no. 2, leg no. 5, the reduction of circulation occurs about 10 s earlier. In this context, it can not clearly be said whether this effect is produced by atmospheric conditions or the motion of the DLC flaps.

Also the configuration 11 shows in the development of the circulation a very small discrepancy to the baseline configuration. As already shown for the configuration 07, the circulation seems to decrease stronger with the wind direction 330°. Apart from that, the measurement date are very closed (Fig. 9).

This observation continues for the configuration 16. At wind direction 330° the decrease of the circulation is stronger than at wind direction 150°, but there is no significant deviation from the baseline configuration (Fig. 10).

The second parameter, which was measured with the LIDAR facility, is the sinking rate of the vortex system. Figure 11 shows the descent of the vortex for the baseline configuration. The differentiation here is also done with the wind direction. Except for flight no. 1 one can see no significant descent characteristics of the vortices. The sinking of the vortex at flight no. 1 is clearly resulted from atmospheric influence. An outlier in the trajectory of the vortex can be observed at flight no. 4. The reason for that is with high probability in the thermal conditions on afternoon.

A very small effect may be obtained at configuration 07 with wind direction 330°. If flight no. 3, leg no. 3 is taken as a reference the descent of the vortex is about 40 m. But in comparison with flight no. 1, leg no. 1 there is no difference between bot trajectories so it has to be asked if also here only atmospheric influence plays a role for this effect. At wind direction 150° the impact is more significant. Here, the descent of the vortex is of magnitude 40 m (Fig. 12).

The configuration 11 shows at wind direction 150° no impact of the deflected aileron and the periodically moved DLC flaps at all. At wind direction 330° one can see although a descent of the vortices but the trajectory of the vortex is going up immediately so this effect is probably caused by thermal wind (see Fig. 13).

A similar characteristic of the sinking trajectory is observable at configuration 16. Also here, there is no effect at wind direction 150°, but at wind direction 330° there is a small deviation from the measurement data of the baseline configuration. Fig. 14 shows the details.

The second part of the analysis deals with the distribution of the relative occurence of the vortex segments. Figure 15 shows some screenshots of the video tape. It is clearly observable that the smoke track and with it the vortex is consistently interrupted. Initially, it is not evident, if the reason for these gaps are atmospheric disturbances or directly the motion of the DLC flaps.

It is expectable that at configurations, which follow the OFS concept, an accumulation of that vortex segment lengths occurs which correlates with the velocity of the vortex generating aircraft and the triggering frequency. At v = 80 m/s und f = 0.5 Hz this should be the length 160 m and whose low-order harmonics (320 m and 480 m). Figure 16 shows the comparison of the baseline configuration with the configuration 07. At the baseline configuration one can see a distribution of relative occurence which is similar to a kind of Gamma distribution. Here, it is conspicuous that in the range from 60 m to 120 m there is a gap in the occurence distribution. This gap occurs at all configurations which have been performed in this flight test. Obviously, there is no vortex segment with such lengths. The reason for that is unknown at the moment. A small accumulation of the segment lengths in the regarding sections one can see at configuration 07. But this is slightly distinct due to the fact that the vortex instability is only weakly triggered by the midboard and inboard DLC flaps.

At configuration 11 there is an effect visible concerning the accumulation of vortex segment lengths (Fig. 17). In contrast to the baseline configuration one can see a kind of a rectangular distribution. This means that all lengths of the vortex segments appear with similar probability. Furthermore, the total number of single incidences is clearly small so that the force of expression of this analysis is reduced.

However, a strong effect is observable at configuration 16 (Fig. 18). Here, all DLC flaps and the ailerons are symmetrically and periodically

deflected. This leads to the conclusion that the influence on the vortex instability is most strong for this configuration. One can clearly see that there is a significant accumulation in the length scales 160 m, 240 m, 320 m and 480 m.
The results of the LIDAR measurements hardly provides a hint to an effect which indicates a significant vortex decay
In nearly all cases the measurement data for the circulation as well as the sinking rate are very closed. At those series of measurement which provides a difference between the baseline configuration and the DFS/OFS or the OFS configuration respectively it is supposable that atmospheric influence played a role. To make a definite statement it is necessary to repeat the experiment at better weather conditions with a larger number of flights.
However, concerning the statistical analysis of the length scales of the vortex segments one can observe that there is a somehow natured influence of the motion of the aileron and the DLC flaps. This is evident at configuration 16. Here, the accumulation of certain lengths of the vortex segments seems to be a hint for the fact that the ring structures which are characteristic for the triggering of the Crow instability are developed. This is also directly visible in the video tapes. However, this must be go along with a distinct decrease of the circulation which could not be detected from the LIDAR data.
Additional to the analysis of measurements some words should have been said about the subjective feeling concerning the flight behaviour of the aircraft during the experiment. At the baseline configuration and the configuration 07 there is no pitching movement of the aircraft which varies from the normal aircraft motions. A small pitching motion is sensible at configuration 11, if the motion of the aircraft is not superposed by atmospheric disturbances. If the test conditions are switched to configuration 16, a strong pitching motion in the range of ±1° is observable. This motion clearly superposes the wind induced motion of the aircraft and could be a considerable problem for sensitive passengers.

V. Conclusion

In spite of the limitations concerning reconstruction work on smoke pod (speed limitation) and co-rotating movable ailerons there is an effect observable which is based most likely on the periodic movement of flaps. There were some test flight runs, on which the development of ring structures or half ring structures respectively became visible. That could be an indication that in these cases the Crow instability is successfully triggered.

VI. References

[1] E. Stumpf, “Investigations of 4-Vortex Systems for an Alleviation of Vortex Wakes and its Realization with Transport Aircraft”, Doctoral Thesis RWTH Aachen, 2004

[2] Eike Stumpf et al., “ATTAS Smoke Try Out Test”, AWIATOR Technical Report 1.1.3-31

[3] Guido Voss, “Premature decay of wake vortices with Differential- and Oscillating Flap Setting”, European Conference on Computational Fluid Dynamics, Egmont aan Zee, The Netherlands, 2006

VII. Figures and Tables

Config	$\eta_{aileron}$ in °	η_{DLC1} in ° outboard	η_{DLC2} in ° midboard	η_{DLC3} in ° inboard	frequency in Hz	Flight No.
Baseline	0,0 / 0,0	0,0 / 0,0	0,0 / 0,0	0,0 / 0,0	---	1,2,3,4
07 (DFS/OFS)	0,0 / 0,0	7,5 / 7,5	7,5 / 0,0	-8,0 / 0,0	0,5	1,2,4
11 (DFS/OFS)	8,0 / 8,0	8,0 / 8,0	8,0 / 0,0	-8,0 / 0,0	0,5	3,4
16 (OFS)	10,0 / 0,0	8,0 / 0,0	-8,0 / 0,0	-8,0 / 0,0	0,5	1,2,4

Tab. 1: List of investigated configurations

Fig. 1: ATTAS (left) and Falcon (right) at DLR Oberpfaffenhofen

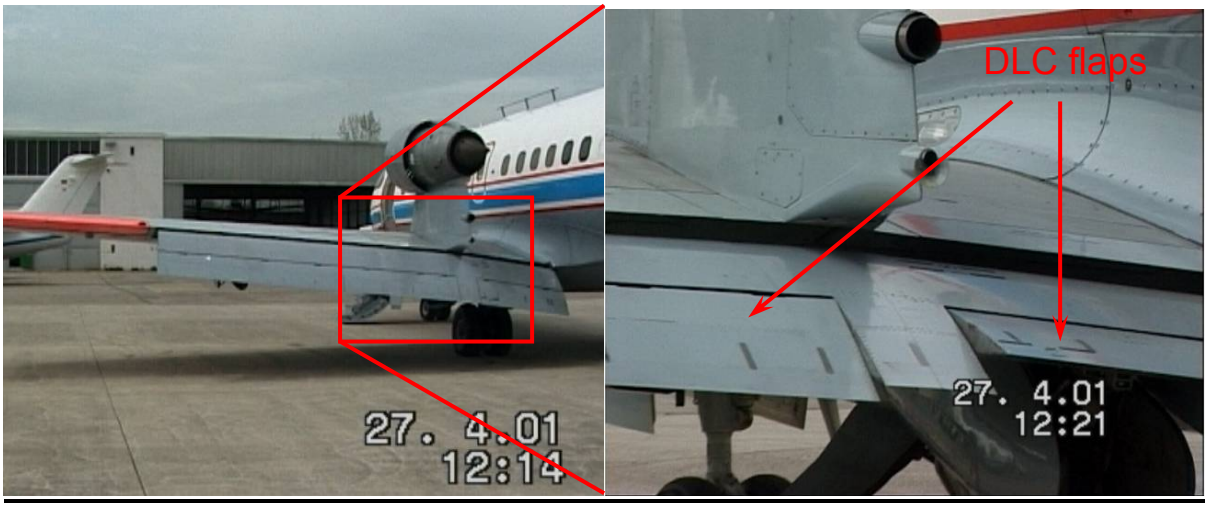

Fig. 2: DLC flaps, integrated within main flap

Fig. 3: Smoke pod in ground test (left) and during flight (right)

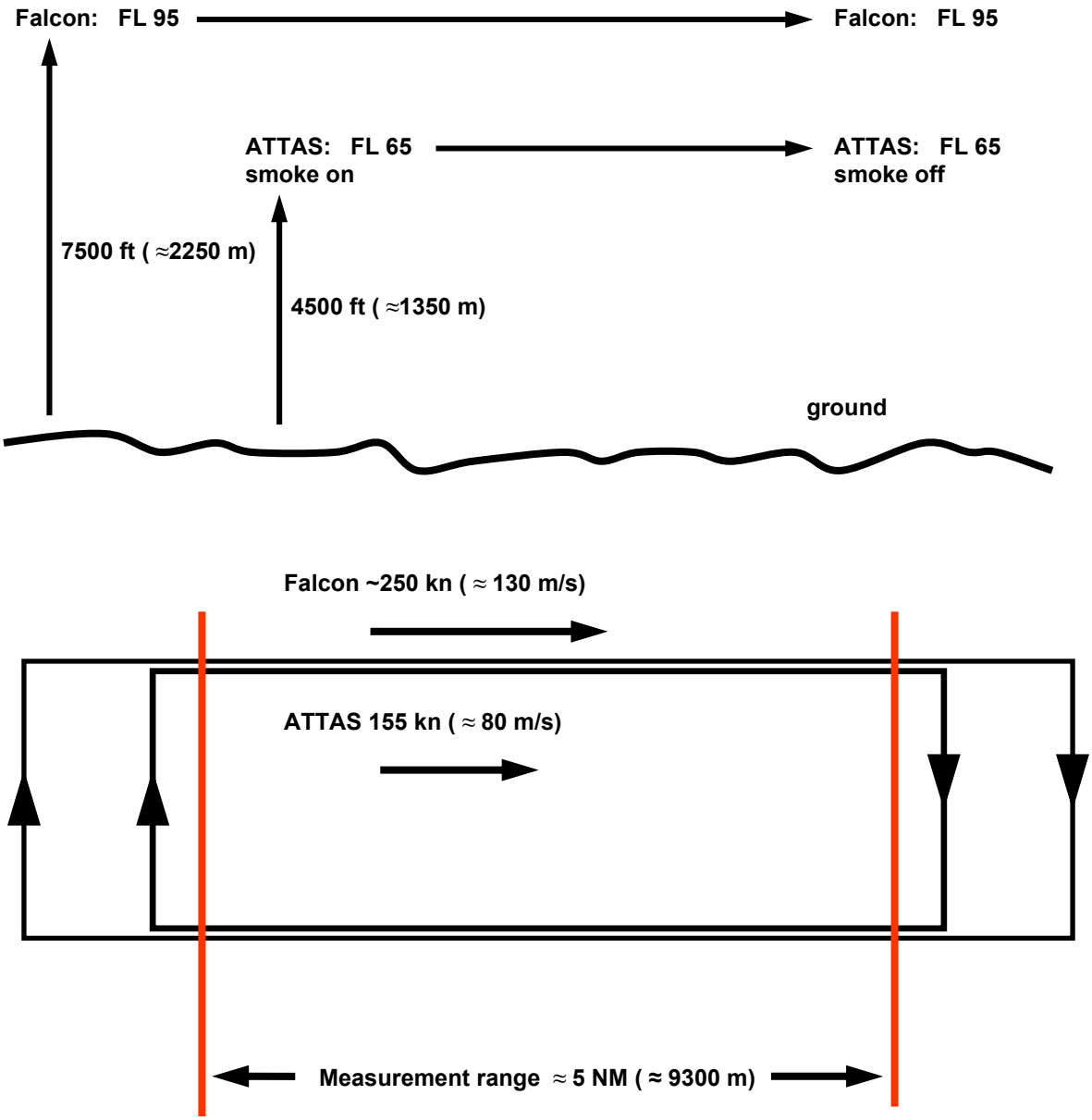

Fig. 4: Schematic view of the flight pattern

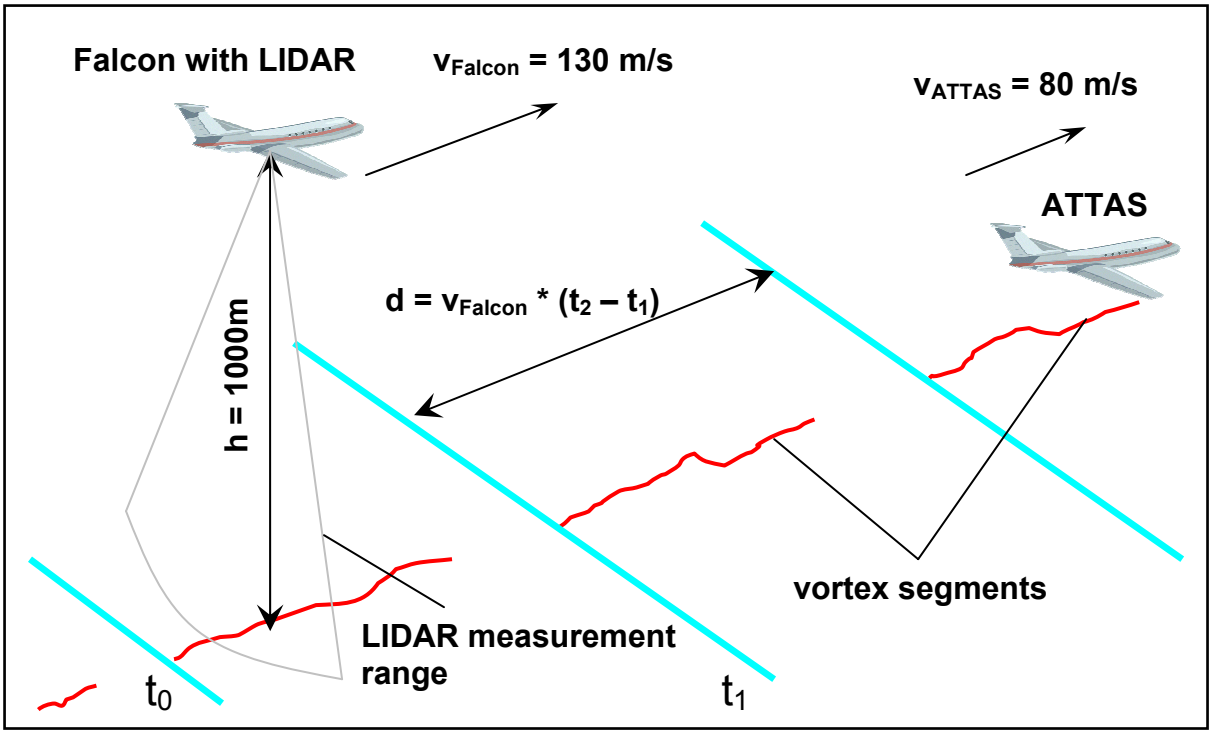

Fig. 5: Schematic test setup for video analysis

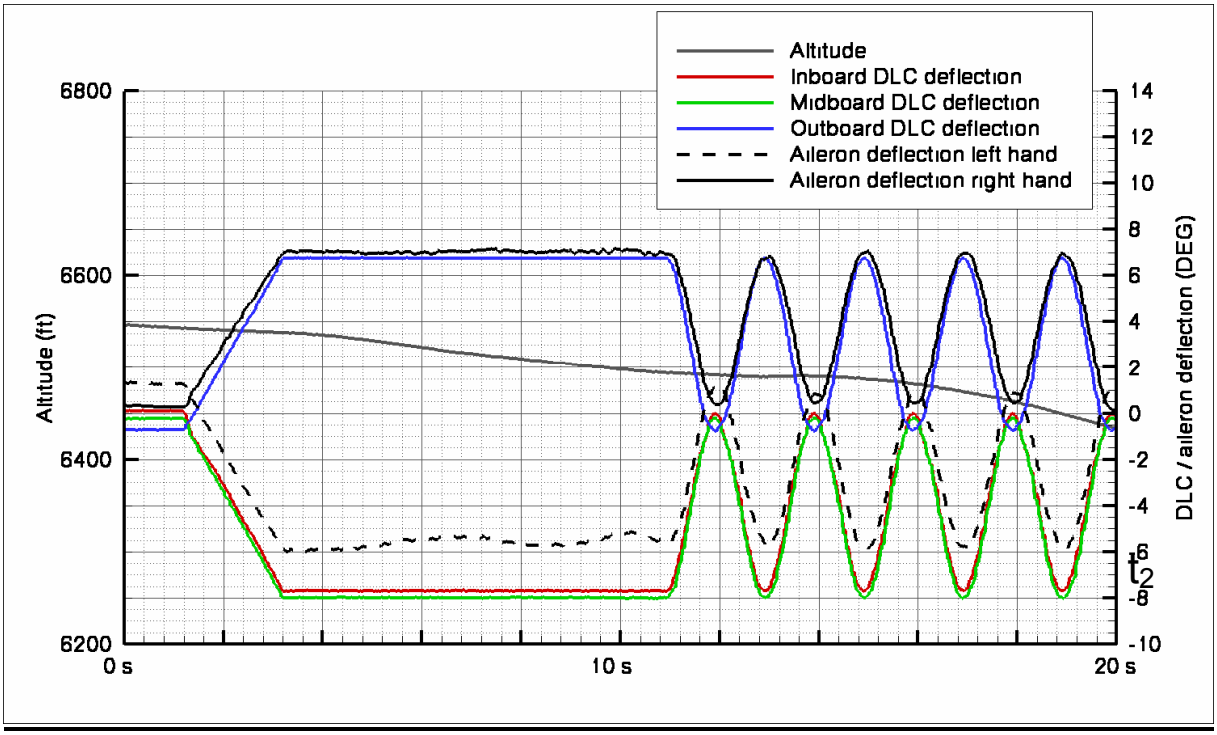

Fig. 6: Motion of flaps and aileron, altitude for configuration 16

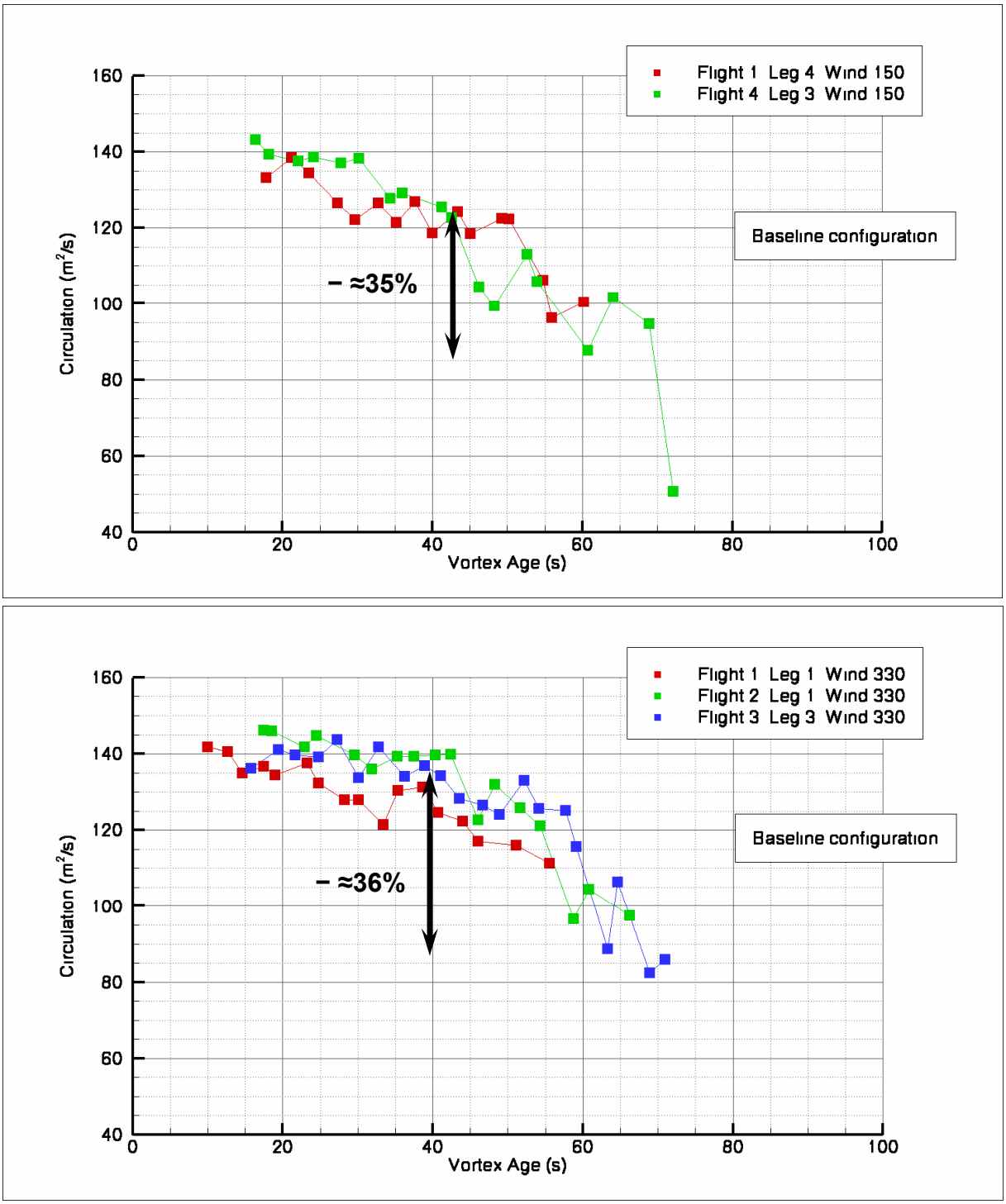

Fig. 7: Circulation of the vortices at baseline configuration

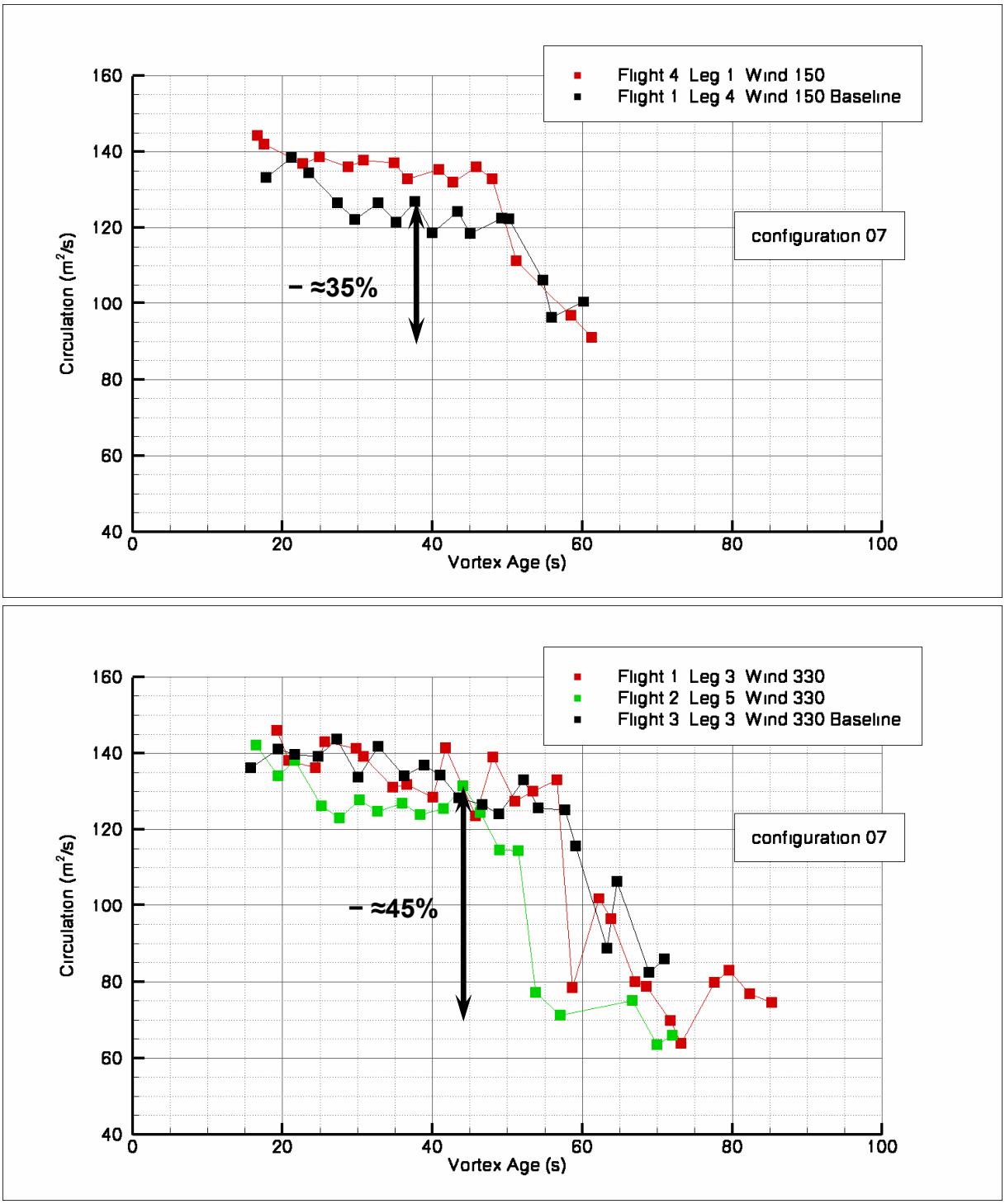

Fig. 8: Circulation of the vortices at configuration 07

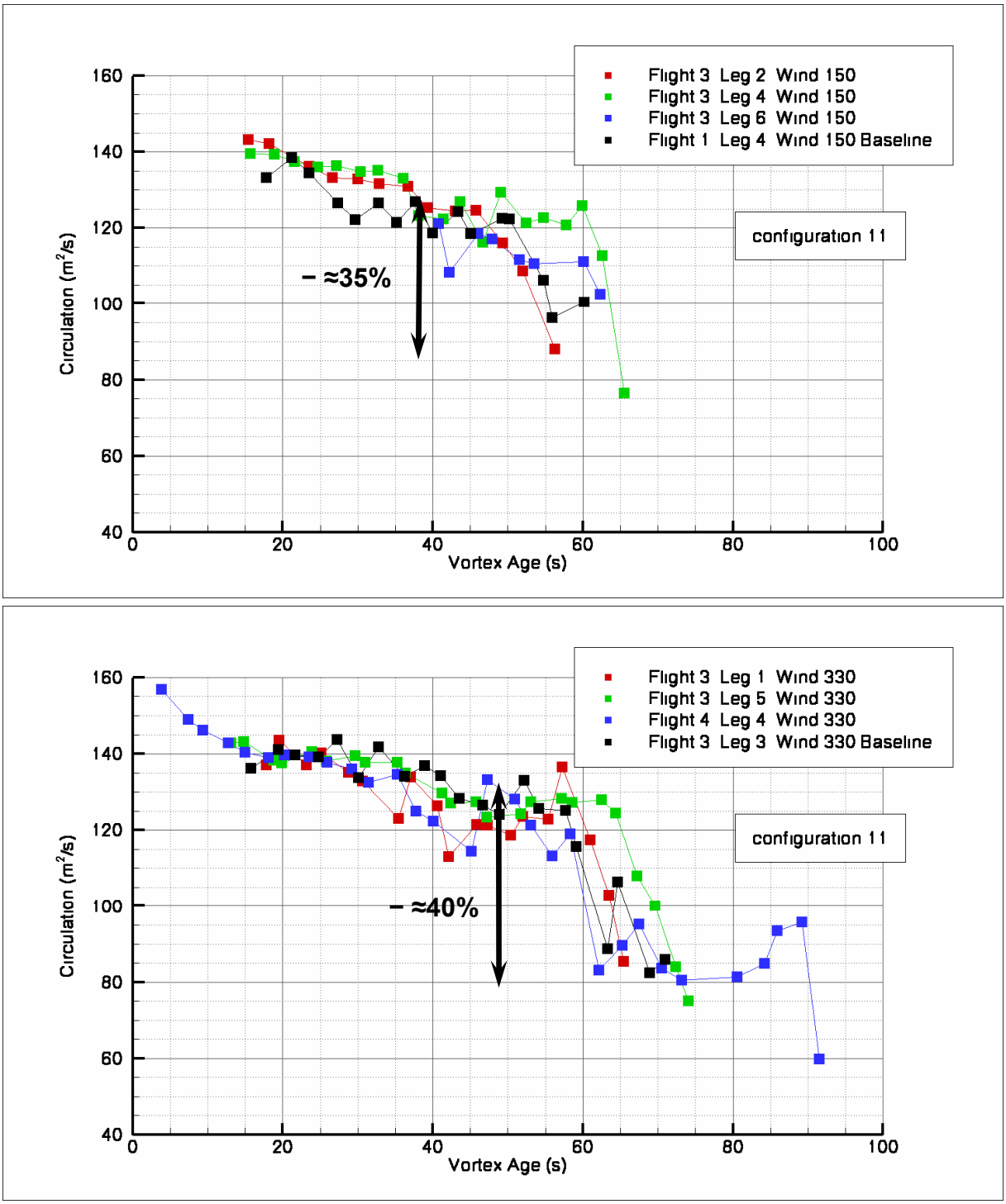

Fig. 9: Circulation of the vortices at configuration 11

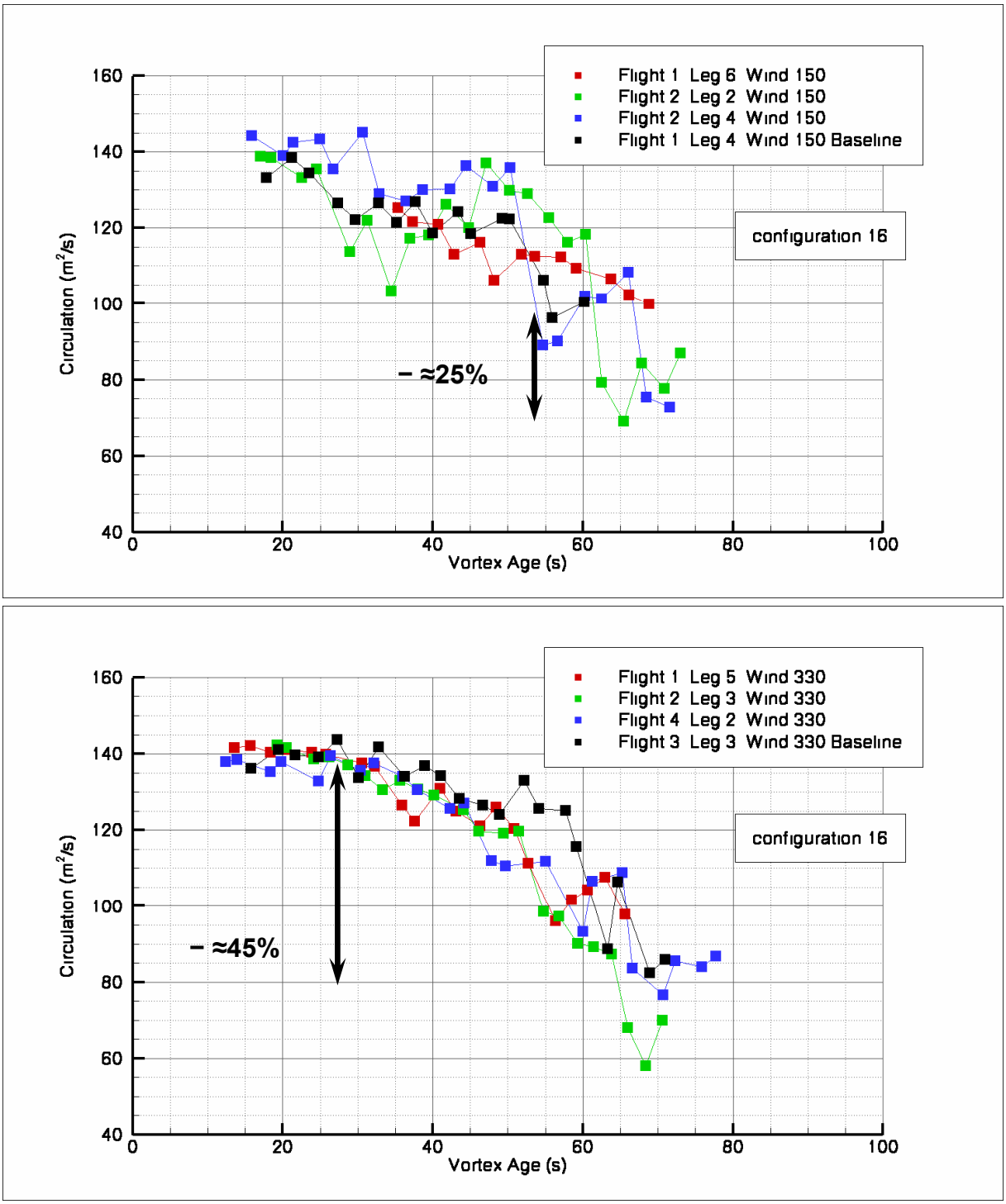

Fig. 10: Circulation of the vortices at configuration 16

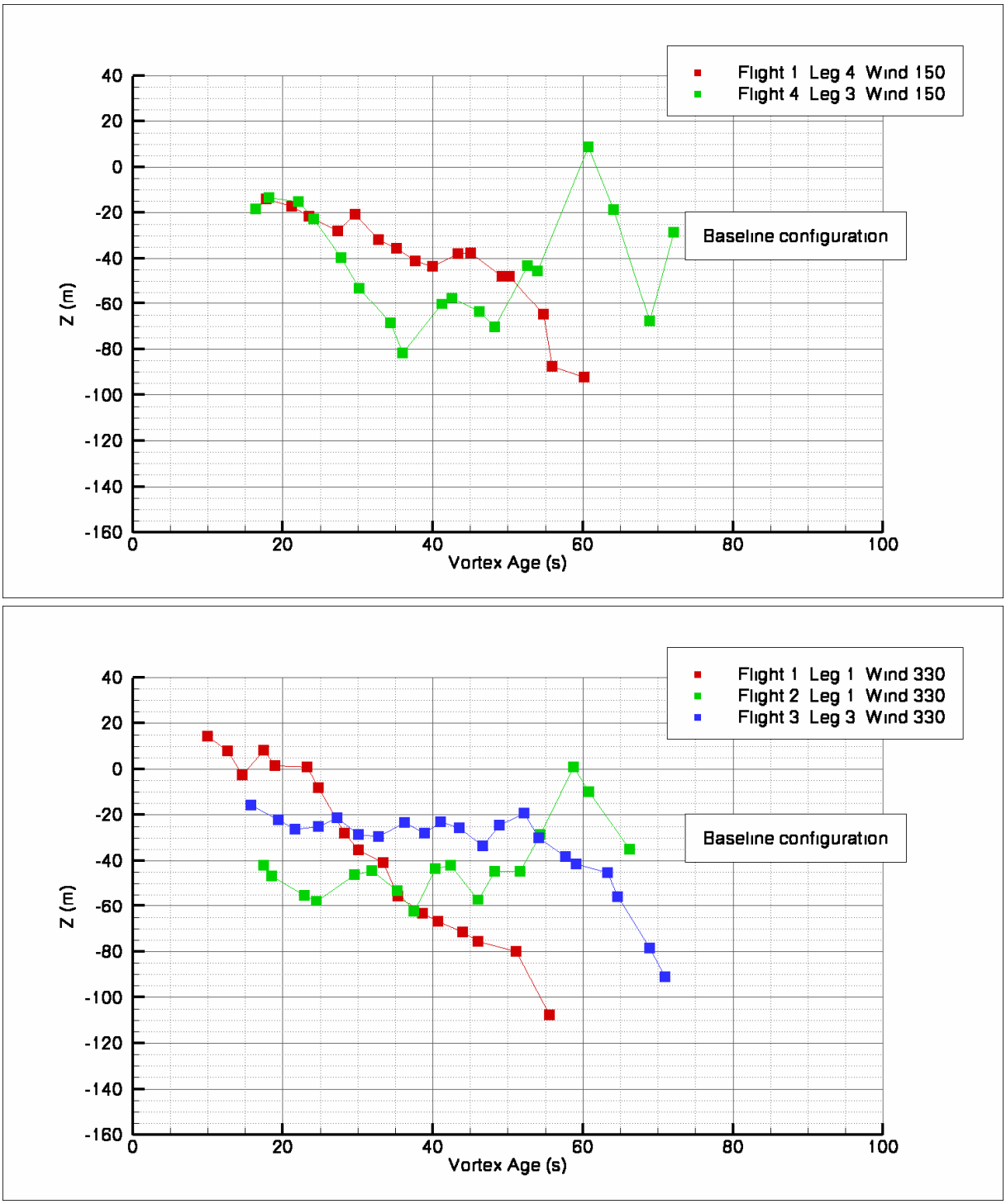

Fig. 11: Downward motion of the vortices at baseline configuration

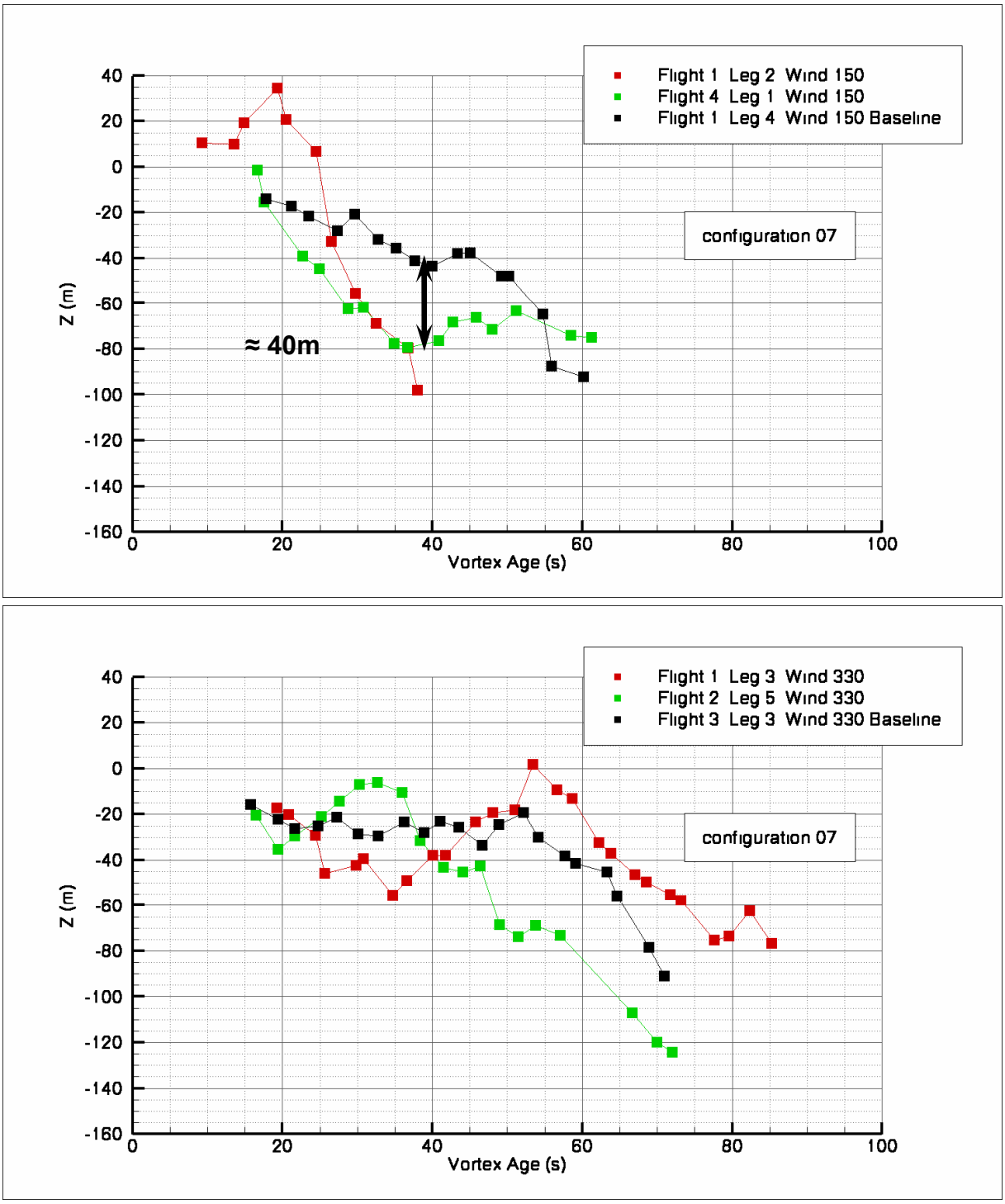

Fig. 12: Downward motion of the vortices at configuration 07

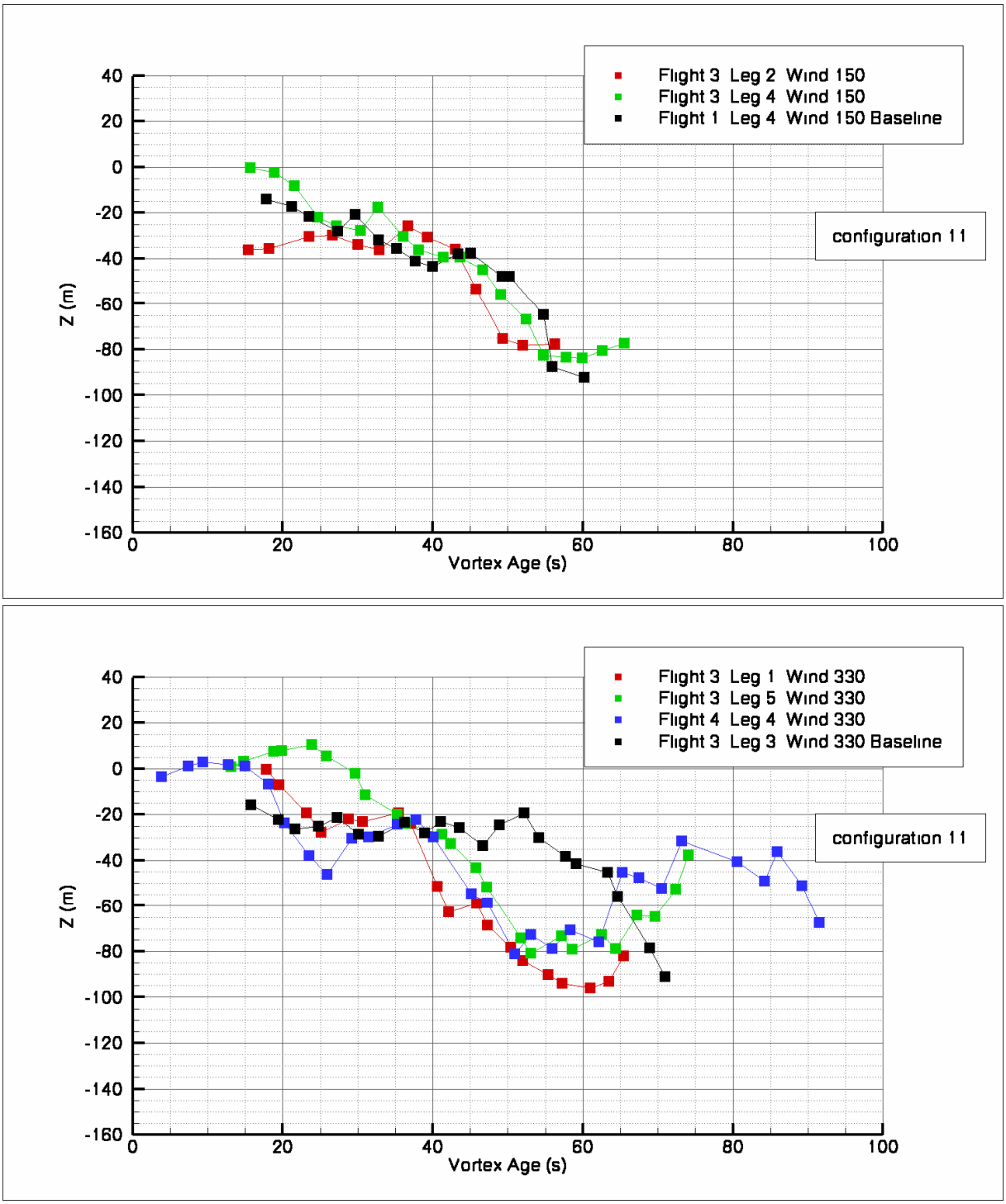

Fig. 13: Downward motion of the vortices at configuration 11

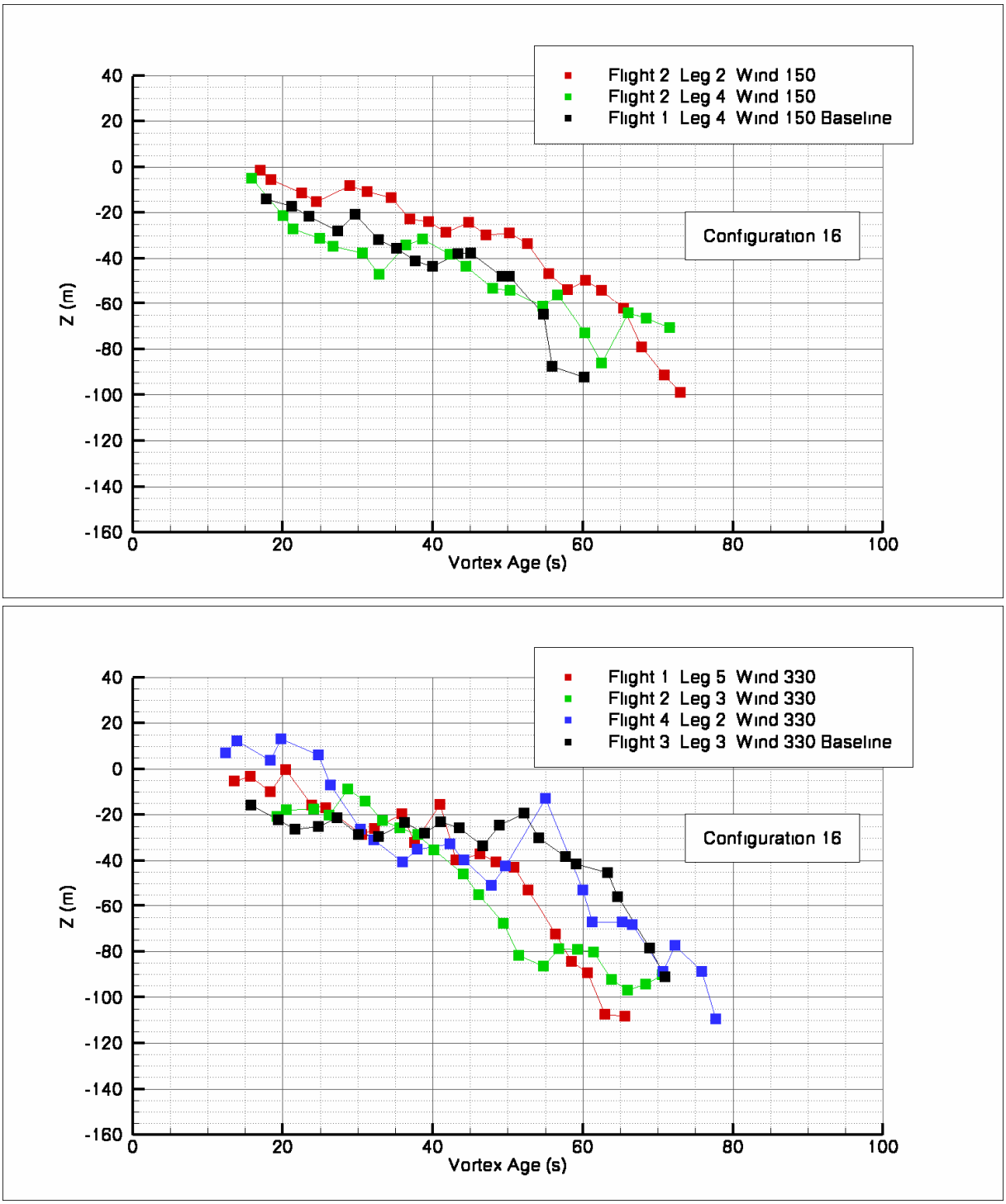

Fig. 14: Downward motion of the vortices at configuration 16

Fig. 15: Screenshots of video from test flight; development of ring structures, ATTAS

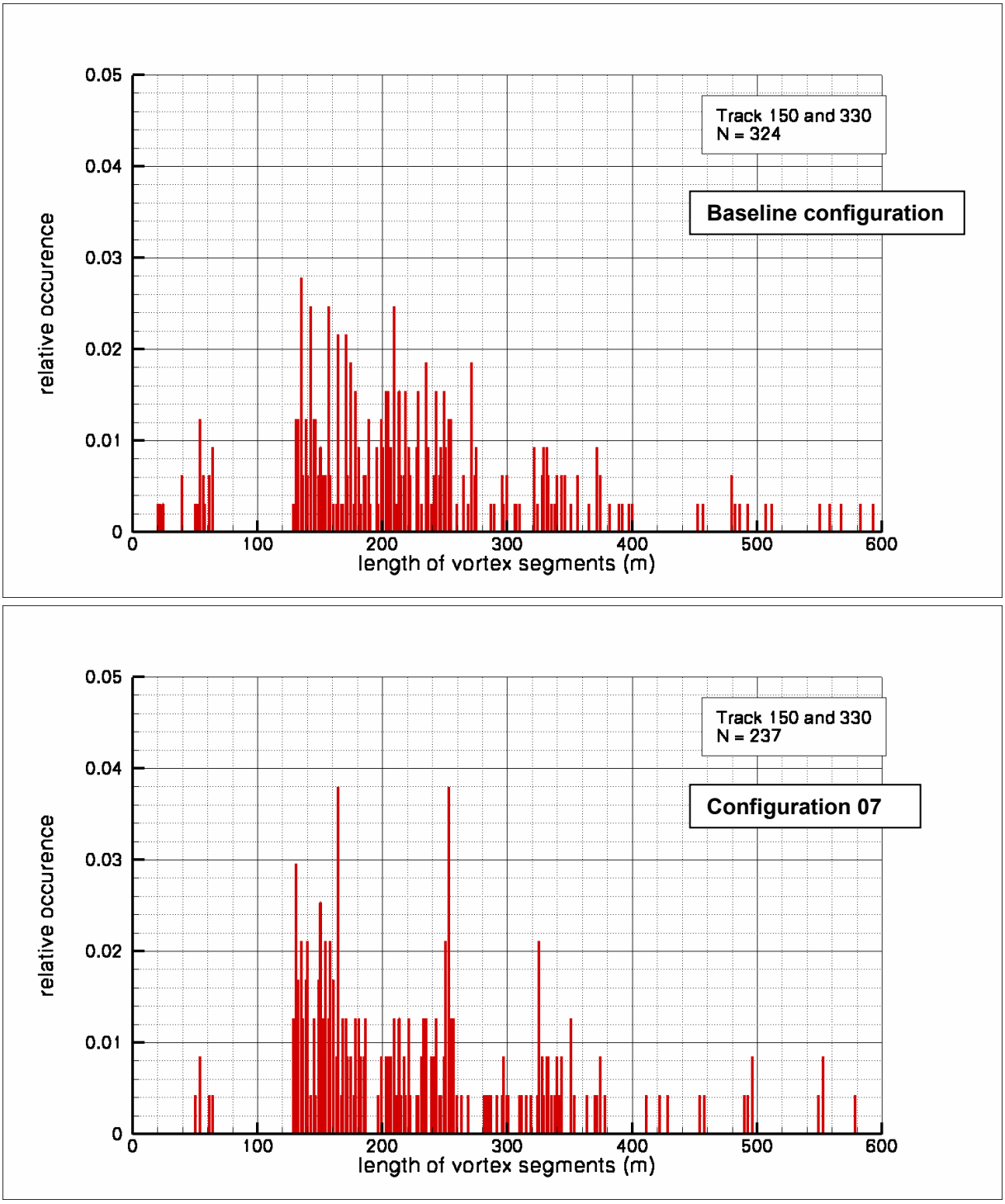

Fig. 16: Comparison of the relative occurence of the vortex segment length between baseline configuration and configuration 07

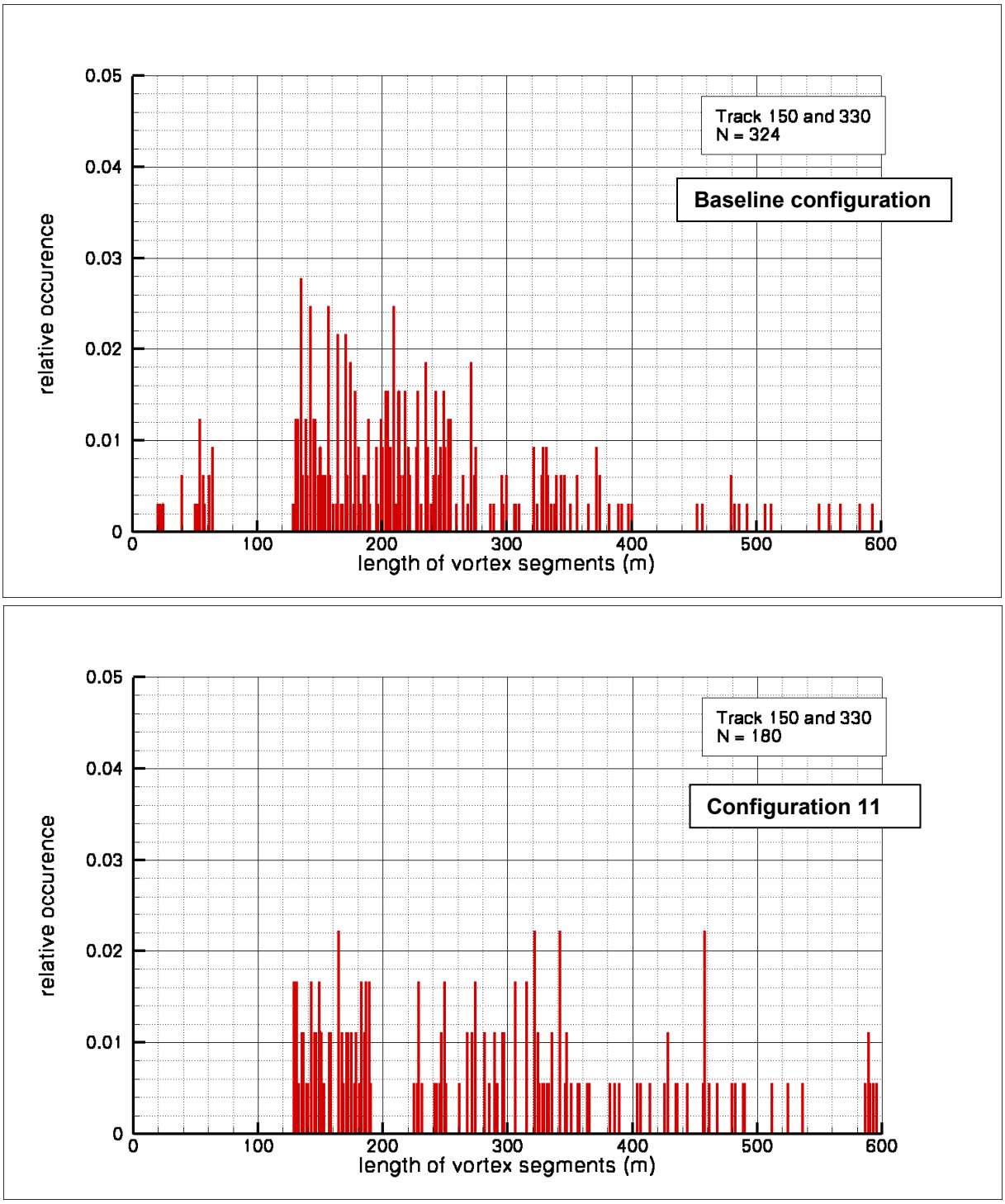

Fig. 17: Comparison of the relative occurence of the vortex segment length between baseline configuration and configuration 11

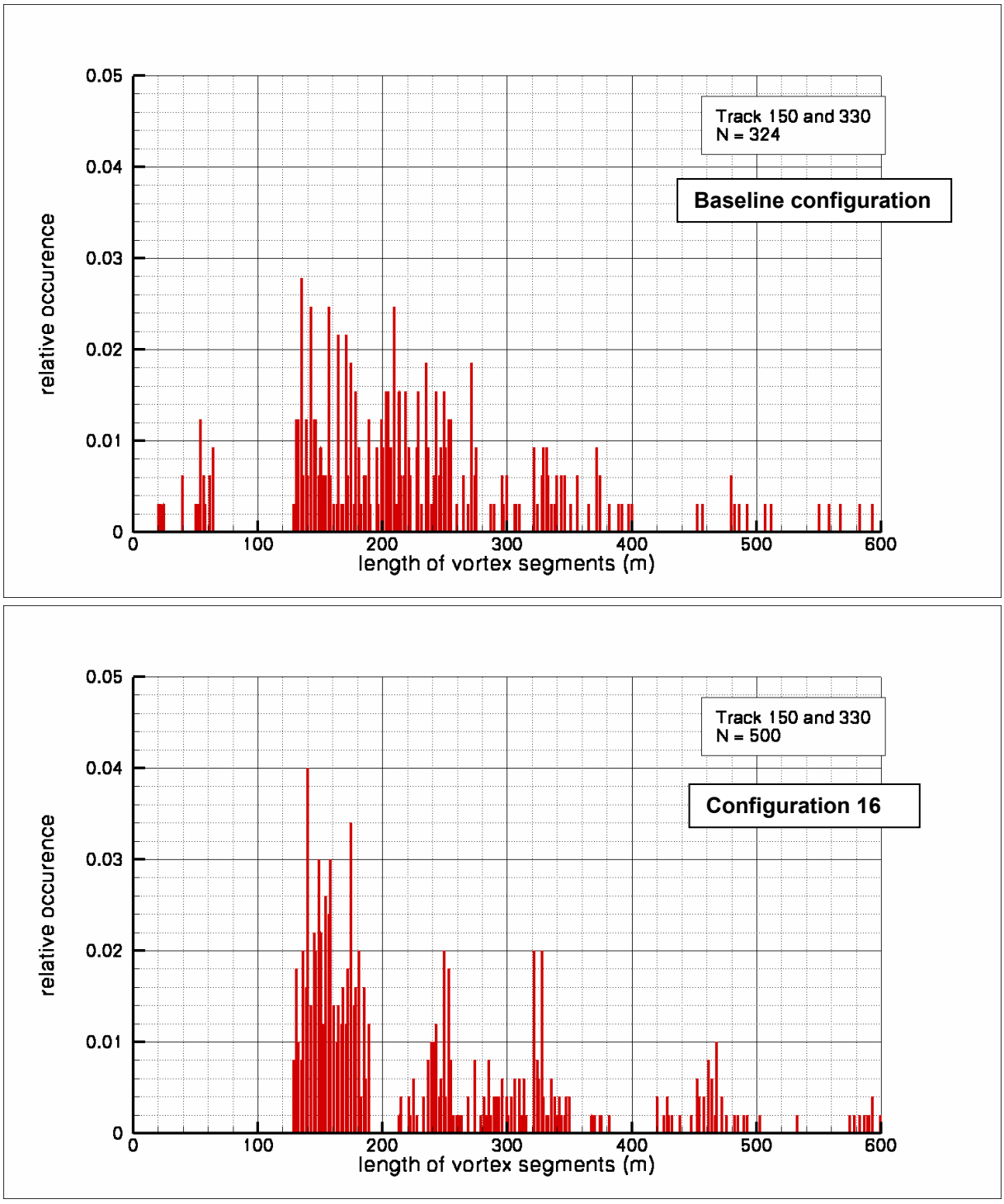

Fig. 18: Comparison of the relative occurence of the vortex segment length between baseline configuration and configuration 16